HHS Public Access

Author manuscript

Oncogene. Author manuscript; available in PMC 2016 December 11.

Published in final edited form as:

Oncogene. 2016 December 08; 35(49): 6309–6318. doi:10.1038/onc.2016.161.

A CCL8 gradient drives breast cancer cell dissemination

Elena Farmaki[1], **Ioulia Chatzistamou**[2,3], **Vimala Kaza**[1], and **Hippokratis Kiaris**[1,4,*]

[1]Department of Drug Discovery and Biomedical Sciences, University of South Carolina, SC, USA

[2]Department of Pathology, Microbiology and Immunology, University of South Carolina School of Medicine, SC, USA

[3]Department of Basic Sciences, Dental School, University of Athens, Athens, Greece

[4]Department of Biochemistry, University of Athens Medical School, Athens, Greece

Abstract

The migration of cancer cells towards gradients of chemoattractive factors represents a potential, yet elusive, mechanism that may contribute to cancer cell dissemination. Here we provide evidence for the maintenance of a gradient of increasing CCL8 concentration between the epithelium, the stroma and the periphery that is instrumental for breast cancer cells' dissemination. In response to signals elicited by the neoplastic epithelium CCL8 production is enhanced in stromal fibroblasts at the tumor margins and in tissues at which breast cancer cells tend to metastasize such as the lungs and the brain. Manipulation of CCL8 activity influences the histology of the tumors and promotes major steps of the metastatic process such as invasion to adjacent stroma, intravasation and ultimately extravasation and seeding. These findings exemplify how gradients of chemoattractive factors such as CCL8, drive metastasis and suggest that interference with their operation may provide means for breast cancer management.

Keywords

Stroma; microenvironment; metastasis; gradient; chemoattraction

Introduction

Tumor cell dissemination reflects the collective outcome of multiple events that include the invasion of cancer cells into the surrounding stroma, subsequently their intravasation and entrance into the circulation, and ultimately their extravasation and seeding into sites of secondary growth[1, 2]. The role of the stroma in these processes is being increasingly appreciated as it establishes positive feedback loops with the neoplastic component of

*Correspondence: Hippokratis Kiaris PhD, Department of Drug Discovery and Biomedical Sciences, University of South Carolina, CLS 713, 715 SUMTER STREET, COLUMBIA SC 29208-3402, Phone: 803 3611 781, kiarish@sccp.sc.edu.

Disclosure statement: The authors have nothing to declare.

Conflict of interest

The authors declare no conflict of interest.

tumors inducing epithelial-mesenchymal transition (EMT) and promoting invasion[3, 4, 5, 6, 7]. In turn, EMT provides a stochastic mechanism by which cancer cells, by acquiring enhanced motility, increase their likelihood to invade adjacent tissues[8]. In addition to random cell migration, directed cell migration towards specific gradients of chemokines, cytokines and growth factors may also contribute to the spread of cancer cells and the initiation of the metastatic process as recognized more than 15 years ago following the description of the CXCL12/CXCR4 paradigm and its role in breast cancer metastasis[9]. However, the contribution of the epithelium in the maintenance of such gradients remains inadequately understood. We hypothesized that soluble factors produced by the stroma in response to signals elicited by the epithelium may facilitate the establishment and maintenance of gradients that could trigger the directional migration of the cancer cells promoting their dissemination. It is conceivable that these gradients may operate both within the tumor microenvironment driving the invasion of cancer cells into the surrounding stroma, and towards the systemic circulation promoting intravasation and establishment of populations of circulating tumor cells (CTCs). Ultimately, local production of chemoattractive factors in distal tissues may promote seeding of CTCs and establishment of metastatic foci.

In order to explore these hypotheses we used breast cancer cells as a model and focused on a conserved chemokine cluster located in chromosomes 11C in mice and 17q12 in humans. This cluster harbors several chemoattractive cytokines many of which previously have been associated with tumorigenesis primarily through generation of a tumor-promoting proinflammatory microenvironment (Figure 1a, refs 10, 11, 12).

Results

Cancer cells activate CCL8 expression in fibroblasts by paracrine mechanisms

To test if stromal fibroblasts are responsive to epithelium-derived signals we exposed mouse 3T3 and human HFFF2 fibroblasts to conditioned media from the metastatic human triple negative breast cancer (TNBC) cells MDA-MB-(MDA)231 and MDA-MB-(MDA)468 and monitored the expression of chemokines CCL1, CCL2 (MCP-1, monocyte chemoattractant protein 1), CCL7 (MCP-3), CCL8 (MCP-2), and CCL11 in both mouse and human cells as well as CCL13 in human and Ccl12 in mouse cells. CCL13 is a human-specific while Ccl12 is a mouse-specific cytokine. As shown in Figure 1b CCL7 was induced only in human fibroblasts and Ccl11 in mouse fibroblasts only, with CCL8 being stimulated in both mouse and human cells. Thus, we focused on CCL8, a chemoattractive cytokine that signals through multiple receptors including CCR1, CCR2B, CCR5 and CCR8[13, 14, 15] in mouse and/or human cells. CCL8 emerges as a good candidate for promoting oncogenesis for several additional reasons: It has been shown that breast cancer cells can activate CCL8 production in adjacent stromal fibroblasts[16]. CCL8 has also been identified by proteomic analyses as a stroma-derived protein in human colon cancers[17] while its levels were significantly elevated in the plasma of breast cancer-prone mice during disease progression[18]. In addition, in a recent study, CCL8 expression has been shown in the melanoma microenvironment[19].The importance of CCL8 in mammary tumorigenesis is also supported by breast tumor expression data (Oncomine, https://www.oncomine.org) showing elevated expression of this cytokine in the stroma of breast tumors as compared to controls

(Figure 1c, ref 20). Furthermore, high CCL8 expression in tumors (Kaplan-Meier-plotter [Breast Cancer] www.kmplot.com/[21], Cancer Genomics Browser, University of California at Santa Cruz, https://genome-cancer.ucsc.edu/) is associated with worse prognosis in breast cancer patients (Figure 1d, Supplementary Figure S1). Noteworthy, this pro-oncogenic role of CCL8 appears to be specific for breast and also cervical cancers because in tumors of other anatomical sites, such as those of colon, pancreas, lungs and others did not show association with disease outcome (Supplementary Figure S1).

The ability of breast cancer cells to stimulate CCL8 in fibroblasts was not retained for all breast cancer cells: When fibroblasts were exposed to media from a panel of breast cancer cells only those from TNBCs MDA231 and MDA468 cells were stimulatory while media from the estrogen-dependent MCF7, BT474, and T47D were not, for either CCL8 (Figure 1e) or CCL7 (data not shown). An intriguing possibility is that in breast cancer cells estrogen-independency is linked to the production of soluble factors that can stimulate CCL8 expression in adjacent fibroblasts, “educating” stroma in a pro-oncogenic manner. Consistently with this notion, the ability of TNBCs and estrogen-positive cancers to “educate” differentially stromal cells has been demonstrated[11, 22, 23]. The profile of CCL8-inducibility was overlapping in human and mouse cells implying the conservation of the breast cancer cell-derived factors between humans and mice since human cell derived-factors could operate effectively onto mouse cells eliciting responses of similar pattern and magnitude (Figure. 1e). Mouse breast cancer cells (4T1 and EO771) were incapable of stimulating CCL8 expression in either 3T3 or HFFF2 fibroblasts under these conditions while prolonged conditioning of media, for 4 days, was stimulatory (data not shown). Of those two mouse breast cancer lines used, EO771 is estrogen receptor positive[24] which is in line with the inability of human cells to stimulate CCL8 in fibroblasts. However 4T1 is considered a model of triple negative breast cancer[25] which contrasts the behavior of human breast cancer cells, a discrepancy that implies intrinsic differences in the biology of human and mouse breast cancers.

CCL8 attracts breast cancer cells *in vitro*

Given the strong chemoattractive activity of CCL8 for immune cells[26, 27], we asked if this chemokine is able to attract breast cancer cells. As shown in Figure 2a, both mouse and human CCL8 attracted breast cancer cells of either mouse or human origin, but not fibroblasts. Furthermore, human and mouse CCL8 are functionally interchangeable because they could reciprocally attract mouse and human cells. This ability of CCL8 to induce the migration of breast cancer cells was also associated with induction in the levels of the mesenchymal marker vimentin which underlines an increase in cellular motility (Supplementary Figure S2). This effect however is not likely associated with the prototypical activation of EMT since slug and snail induction was virtually absent. Considering that CCL8 and other chemokines act primarily on leucocytes that may migrate by amoeboid movements[28], similar effects on breast cancer cells are conceivable. In addition, selection of specific cell populations rather than modification of the cells’ transcriptional program remains also as a possibility. In order to rule out though the possibility that the elevation in cell migration by CCL8 was due to an overall increase in cell motility and not associated with chemoattraction we compared the migration of MDA231

cells in transwells at which CCL8 was placed in the lower chamber versus distributing it evenly between the lower and upper chambers. As shown in Figure 2b cells migrated from lower towards increased CCL8 concentration while migration was not stimulated when equal amounts of CCL8 were maintained between transwells. In addition, human CCL20 had only a minor effect in the migration of MDA231 cells, as it has been previously shown[29] (Supplementary Figure S3).

In order to identify the specific receptors that mediate MDA231 cells' migration towards human CCL8, we hypothesized that the particular MDA231 cells expressing these receptors at higher levels will be enriched in the lower chamber of a transwell following CCL8-induced chemoattraction. Following normalization versus untreated cells in transwells and cells treated with CCL8 in a regular well (no migration and thus no enrichment) we were able to record enrichment of CCR1 and CCR3 (Figure 2c).

The fact that both the stimulus for CCL8 production and the target for CCL8-induced chemoattraction are the cancer cells predicts the establishment of a paracrine loop of repeated cycles of "stromal CCL8 activation-cancer cell attraction". This loop, involves both stromal and cancer cells establishing a self-sustained gradient of CCL8 around the fibroblasts that will progressively stimulate cancer cells' movement (Figure 2d).

Expression profile of Ccl8 in tumors, stroma and peripheral tissues

By using EO771 mouse breast cancer isografts as a model we sought to explore further this hypothesis and the implications of CCL8 - based gradients in tumorigenesis. EO771 cells have originally been derived from breast tumors in C57BL6 mice[30] which permit their inoculation in syngeneic Ccl8-deficient animals[31]. Despite their limited ability to stimulate Ccl8 expression in fibroblasts, we reasoned that EO771 isografts represent adequate system to study the role of a Ccl8 gradient between the stroma and the epithelium because EO771 cells express lower levels of Ccl8 than stromal cells *in vivo* as indicated by the fact that EO771 tumors growing in wt mice had significantly higher Ccl8 levels than tumors growing in Ccl8KO mice (Figure 3a). Thus, increasing levels of Ccl8 can be maintained between the epithelium and the stroma despite that it is not the cancer cells that actively induce and maintain fibroblasts' Ccl8 production. Consistently with the stromal origin of Ccl8, anti-CCL8 immunoreactivity was detected in stromal cells of EO771 tumors, especially at the tumor margins (Figure 3b, Supplementary Figure S4). Noteworthy, a correlation between the levels of circulating Ccl8 in tumor-bearing wt mice and EO771 tumor size was detected (Figure 3c, Supplementary Figure S5) which in association with the inability of EO771 cells to activate Ccl8 expression in 3T3 and HFFF2 fibroblasts was unexpected. In addition, RAW 264.7 macrophages and MEFs did not exhibit elevated levels of Ccl8 when cultured in EO771 conditioned media rendering unlikely that the increased levels of plasma Ccl8 in tumor - bearing mice is due to stimulation of Ccl8 expression in stromal cells (data not shown). In view of the fact that cells of the microenvironment constitute the major source of Ccl8 it is plausible that larger tumors mobilize higher numbers of Ccl8-producing stromal cells than smaller tumors, thus elevating total circulating Ccl8 levels. Indeed, besides the stromal fibroblasts that are abundant in the periphery of EO771 tumors, macrophages that also express Ccl8 are over-represented in tumor margins (Supplementary Figure S6). In

addition, peripheral tissues may also activate Ccl8 production in response to tumor-derived signals, contributing to the increased levels of circulating Ccl8 in the tumor-bearing mice. Measurement of Ccl8 amounts in various organs showed elevated levels of this cytokine in peripheral tissues of tumor-bearing as compared to tumor-free animals (Figure 3d). These tissues included the lungs and the brain that represent common sites of metastatic growth for breast cancers (Figure 3d). In mammary glands the highest amounts of Ccl8 were detected, which despite the fact that their levels were not elevated in the breast tumor-bearing mice they still remained higher than those of the Ccl8 levels in the tumors (Figure 3d). This likely re-enforces the maintenance of the Ccl8 gradient towards the periphery of the tumors and probably contributes to the unique association between breast cancer prognosis and Ccl8 expression.

Consequences of Ccl8 inhibition in the profile of tumorigenesis and histopathology of tumors

Then we asked the consequences of Ccl8 inhibition in tumor onset. First we blocked Ccl8 activity by a neutralizing antibody administered daily for 5 days in wild type C57B6 mice following orthotopic inoculation of the syngeneic EO771 mammary breast cancer cells. As shown in Figures 4a and 4b inhibition of Ccl8 activity only moderately delayed the onset of EO771 breast tumors. Then we tested the effects of genetic ablation of Ccl8 in the onset of EO771 breast tumors. Consistently with the effects of antibody-mediated inhibition, genetic deletion of Ccl8 also modestly delayed the onset of EO771 tumors (Figure 4c). Despite the limited effects in the kinetics of implanted breast tumors, Ccl8 deficiency in the stroma resulted in tumors with increased cellularity, better-defined borders (Figure 4d) and less stroma as indicated by Van Gieson staining for elastic fibers (Figure 4e). Furthermore, vimentin expression close to tumor margins was more intense in the tumors developed in wt than Ccl8KO mice (Figure 4f). Thus, stroma-derived Ccl8 confers characteristics that are associated with the increased ability of cancer cells to disseminate.

CCL8 mediates invasion of breast cancer cells towards adjacent fibroblasts *in vivo*

The histopathology of the tumors with stromal Ccl8 ablation, the chemoattractive activity of Ccl8 onto breast cancer cells and the maintenance of a Ccl8 gradient between the stroma and the epithelium are in line with a stimulatory role for this cytokine in the metastatic potential of the cancer cells. Attempts to detect CTCs in the blood or metastatic foci in the lungs of EO771 tumor-bearing wt or Ccl8KO mice resulted only in their marginal detection in the wt animals, at levels though below those permitting comparison between experimental groups. Thus we utilized the highly metastatic MDA231 human breast cancer cell line and manipulated either directly or indirectly CCL8 levels in tumor-bearing animals in order to reveal evidence of differential metastatic potential. As described above MDA231 cells are highly sensitive to CCL8-induced chemoattraction and efficiently stimulate fibroblasts' CCL8 production by a paracrine manner. In addition, when MDA231 cells were implanted orthotopically in *nude* mice, Ccl8 levels were stimulated in peripheral tissues in a manner exhibiting the same pattern with that recorded when EO771 cells were implanted in C57BL6 wt mice (Figure 5a vs. 3d). In addition, mouse Ccl8 levels in the serum increase in association with tumor size, further confirming the ability of MDA231 cells to activate the production of Ccl8 in the host (Supplementary Figure S7). Thus, they constitute an adequate

system to study the role of stroma-derived Ccl8 in breast cancer. Initially we sought to explore if fibroblast-derived CCL8 can drive invasion of cancer cells to adjacent stroma. To attain this, CCL8 expression should be stimulated in stromal fibroblasts in the vicinity of the tumors and then it should be able to attract the cancer cells triggering their dissemination. To test this, HFFF2 fibroblasts were enclosed in matrigel and inoculated s.c. in mice close to MDA231 tumors or in tumor-free mice (Figure 5b). As shown in Figure 5c, in line with the conditioned media-based experiments described in Figure 1, HFFF2 fibroblasts close to cancer cells exhibited elevated expression of CCL8 as compared to fibroblasts that had been inoculated in tumor-free mice. Then, we recorded the invasion of MDA231 cells towards the HFFF2 matrigel nodules and found that it was stimulated by a manner that is CCL8-dependent since treatment of mice with a neutralizing antibody for CCL8 blocked their invasion (Figures 4d–f). Thus *in vivo*, CCL8 that is triggered in fibroblasts in response to signals elicited by breast cancer cells guides their invasion to adjacent stroma.

CCL8 induces extravasation of breast cancer cells

The chemoattractive activity of CCL8 predicts that elevated levels of CCL8 in the blood may also stimulate intravasation of the cancer cells[32, 33]. The existence of CTCs is a pre-requisite of hematogenous metastasis and their number represents a good reflection of the pro-metastatic activity of tumors[34, 35]. To that end, we measured the number of circulating tumor cells (CTCs) in mice bearing MDA231 tumors following i.v. administration of hCCL8. After 24h, CTCs were evaluated by qPCR for human cytokeratin 19 by using total RNA from PBMCs as template, the amount of which had been normalized for mGAPDH. As shown in Figure 5g, hCCL8 effectively stimulated the extravasation of MDA231 cells and increased their abundance in the blood, which is in line with a prometastatic role for this cytokine.

CCL8 promotes seeding of breast cancer cells in the periphery

Since CCL8 operates as a chemoattractant it is conceivable that tissues with elevated levels of CCL8 would attract more efficiently breast cancer cells facilitating their seeding and the development of sites of secondary growth. Therefore, MDA231-β-Gal cells were injected i.v. in nude mice and the efficiency of seeding in the mammary glands, that express high Ccl8 levels, was evaluated (Figure 5h). As shown in Figure 5i MDA231-β-Gal cells colonized the mammary glands by a manner that was CCL8-dependent because anti-CCL8 treatment after cancer cell injection nullified the number of the resulting MDA231 foci in the mammary fat pad (Figure 5j, Supplementary Figure S8). A similar trend, albeit insignificant, was also detected in the colonization of the lungs (Supplementary Figure S9). Thus, CCL8 does not only promote intravasation in the primary sites of tumor growth but also extravasation and establishment of secondary growth by enhancing cancer cell seeding.

Discussion

Collectively these findings are consistent with the establishment of a gradient of CCL8 that facilitates the communication between the neoplastic epithelium and the stroma and promotes the motility and directional migration of cancer cells. This CCL8-based gradient is self-sustained because it can be maintained by the constitutive production of the cytokine by the stroma that is more abundant in the tumor margins and is potentiated by signals elicited

by the epithelium. The breast tumor-associated stimulation of CCL8 levels in the lungs and the brain implies that their seeding by circulating breast cancer cells during tumor growth is not merely due to the increased possibilities of larger tumors to metastasize but is a rather dynamic feature sustained by paracrine signals originating from the neoplastic epithelium. Depending on its relative levels in the blood, the tumors and the peripheral tissues, CCL8-like gradients can further mobilize cancer cells by promoting intravasation at the primary site or by triggering extravasation and metastatic seeding at distal locations. The abundance of CCL8 in the normal mammary tissue may contribute to tumor self-seeding that has been described before for breast and other cancers[36]. In this case though it appears that tumor self-seeding is promoted by a stroma-derived factor rather than cancer cell-derived factors[36]. A potential implication of this hypothesis is that field cancerization may not reflect only de novo malignant conversion of the epithelium[37] but also the onset of secondary tumors from cells that have disseminated from the primary tumor and established local outgrowths in the vicinity of the primary tumors or they are due to metastatic foci from cancer cells that had been attracted from the circulation.

In view of the fact that both the genetic and the antibody-mediated inhibition of CCL8 activity interfered with the motility of cancer cells and their invasive/metastatic activities suggest that anti-CCL8 therapy should be considered for the management of metastatic breast cancer. Such approach is not expected to produce considerable adverse effects, as suggested by the absence of visible phenotypes in the CCL8KO mice and the well-tolerated administration of neutralizing antibodies. It is noted that recently the neutralization of CCL2 has been explored for prostate cancer[38, 39].

Although the exact contribution of CCL8 in human breast cancers remains to be determined, these findings exemplify how CCL8-like gradients can drive the metastatic process by promoting invasion, intravasation and ultimately extravasation and seeding into sites of secondary growth (Figure 6).

Materials and Methods

Cell culture

MDA-MB-231, MDA-MB-468, MCF7, 3T3, 4T1, RAW 264.7, HFFF2 cell lines were cultured in DMEM with 10% HyClone FetalClone II serum (Thermo Scientific). BT474, T47D, EO771 cells were cultured in RPMI 1640 medium supplemented with 10% FBS HyClone FetalClone II serum (Thermo Scientific). The C57BL/6-derived breast cancer cell line EO771 was obtained from Dr. Frank C. Marini (Wake Forest School of Medicine, NC). EO771 cells, prior to mice inoculation were tested for viral pathogens and mycoplasma contamination (IDEXX Bioresearch, Columbia, MO). HFFF2 cells were obtained as cryopreserved cells from Sigma-Aldrich and were used in all assays between passage five and ten. All other cell lines were originally obtained by ATCC (Manassas, VA) and subsequently maintained in our laboratory. Most recent authentication was performed one month prior to submission by STR analysis (Biosynthesis, Lewisville, TX). MDA231 cells were transfected with pcDNA3.1-β-Galactosidase expressing plasmid, using TurboFect Transfection Reagent (Thermo Scientific) according to the manufacturer's instructions followed by selection with 1mg/mL G418. All cell lines were frequently tested for

mycoplasma contamination using commercially available Mycoplasma detection kit (Myco Alert kit, Lonza).

Conditioned media

For conditioning of media cells were plated in duplicates on 6 well plates at a starting density of 4×10^5 cells/well for 48 hours. Conditioned media were collected and centrifuged for 5min at 1200 rpm to remove cell debris. Then, 3 mL of the conditioned media were added for 48h in HFFF2 or 3T3 fibroblasts that had been cultured for 16h in serum free media on 6-well plates at a density of 2.5×10^5 cells/well. Experiments were performed at least 3 times each time in duplicates, and similar results were obtained.

Migration assays

10^4 cells were seeded on the top chamber of the transwells (24-well format, with 8 μm pore size insert, Costar) in serum free media and inserted in the plates containing 600 μl of medium supplemented with 10% FBS and the desired concentration of chemoattractant (human or mouse recombinant CCL8, Cellgs, human CCL20, Biolegends) into the lower chamber. After 16 hours the upper sides of transwells were washed in PBS, scraped gently with cotton swab to remove cells that didn't migrate and then cells on the lower side of membrane were fixed with methanol and stained with hematoxylin. Migrated cells were counted under microscope and counts were performed by two independent observers blinded to treatment. For receptors expression, RNA was isolated from migrated cells treated with human CCL8 for 5 hours and also cells that were treated in regular wells under the same conditions. Experiments were performed at least 3 times, each time in duplicates and representative results are shown.

RNA and Protein assays

Total RNA was extracted from cultured cells using RNeasy Mini Kit (Qiagen, Hilden, Germany) according to the manufacturer's instructions. PrimeScript RT reagent kit-Perfect Real Time (Takara Bio, Japan) for RT-PCR was used for cDNA synthesis according to the manufacturer's protocol. Total RNA was extracted from cultured cells and tissues using RNeasy Mini Kit (Qiagen) according to the manufacturer's protocol.

For CTCs detection, peripheral blood samples from mice were obtained from retro-orbital venous plexus sampling in tubes containing EDTA. Red blood cells were lysed using red blood cells lysis buffer and RNA was extracted from PBMCs using RNeasy Micro Kit (Qiagen) according to the manufacturer's protocol. cDNA was synthesized using Maxima First Strand cDNA Synthesis Kit (Thermo Scientific). Real-time quantitative PCR was performed using an Applied Biosystems 7300 real time instrument (Applied Biosystems). RT-PCR product was amplified using the iTaq Universal SYBR Green Supermix (Biorad) in a total reaction volume of 20 μL. Product identity was confirmed by a single pick in the melt curve. Relative expression values were calculated using the $2^{-(\Delta\Delta Ct)}$ formula. The data are presented as fold change in gene expression normalized to GAPDH and relative to the untreated control. Immunohistochemistry was carried out in formalin fixed, paraffin embedded tissue specimens. The antibodies used were rabbit polyclonal anti-MCP2/CCL8 (orb13564), by Biorbyt; 1:100 and rabbit monoclonal [EPR3776] anti-Vimentin (ab92547),

by Abcam; 1:250, rabbit monoclonal [SP115] anti-F/480 (ab111101), by Abcam; 1:250. Immunostaining was performed by using the Dako EnVision+ System-HRP (DAB) (K4041), following the manufacturer's instructions. Negative controls included omission of primary antibody. Before evaluation, a weak counterstaining with hematoxylin was performed in all immunostained specimens. Evaluation of samples was performed blindly. For immunoblot analysis and Elisa CCL8 detection, cells and tissues were solubilized with ice-cold RIPA buffer (Thermo Scientific) supplemented with protease inhibitor cocktail (Thermo Scientific). The protein concentration in the lysates was determined by using Bradford assay (Biorad). Equal amounts of total protein were resolved by SDS-PAGE and immunoblotted with rabbit monoclonal [EPR3776] anti-Vimentin (ab92547), by Abcam and rabbit polyclonal anti-Cytokeratin 18 (ab52948), by Abcam. Plasma, tissues and cells levels of mouse Ccl8 were measured by Mouse CCL8/MCP-2 DuoSet ELISA Development kit (R&D Systems) according to manufacturer's protocol.

Animal studies

Ccl8KO mice were obtained from KOMP Repository (UC Davis, USA) and subsequently bred and maintained at the USC. NCr nude mice were obtained from Taconic. Six- to eight-week-old, female animals were used for all experiments. Animal studies complied with Institutional guidelines. For tumor reconstitution experiments in C57B6 mice, 1×10^5 EO771 cells were resuspended in 0.1 mL of serum-free RPMI and then injected subcutaneously into C57B6 (n=19) or Ccl8KO mice (n=15) (also in C57BL6 background). Animal numbers were determined based on pilot studies and depended on the number of litters for the KO mice. Subsequently, animals were observed daily for tumor development. For antibody treatment, C57B6 mice 6 days after the cell injections, were randomly divided into two groups, the first group (n=10) was treated with mouse monoclonal anti-CCL8 neutralizing antibody (Creative Diagnostics) (16μg per injection) and the second group (n=10) with normal mouse IgG (sc-2025) (Santa Cruz) (16μg per injection). Mice received five daily i.p. injections of anti-CCL8 or IgG. For *in vivo* metastasis assays in nude mice, 3×10^6 MDA231-β-Gal cells were resuspended in 0.1 mL of matrigel and then injected subcutaneously into nude mice. Six days later, 3×10^6 HFFF2 resuspended in 0.1 mL of matrigel were injected next to MDA231-β-Gal matrigel. Three days after fibroblasts inoculation, mice were randomly divided into two groups, the first group (n=5) was treated with mouse anti-CCL8 monoclonal neutralizing antibody (DMABT-H16868) (Creative Diagnostics) (16ug per injection) and the second group (n=4) with normal mouse IgG (sc-2025) (16ug per injection). Mice received three daily i.p. injections of anti-CCL8 or IgG. Mice were sacrificed the next day after the final injection. For CTCs detection, MDA231-β-Gal were injected as described above and then 4 weeks later one group (n=2) received one intravenous injection of human recombinant CCL8 (Cellgs) (1.5μg per injection) and the second saline (n=2). Mice were sacrificed the next day after the final injection. For tumor seeding experiments, 5×10^5 MDA231-β-Gal cells resuspended in 0.1 mL of PBS were injected intravenously into nude mice and 8 hours later they were divided into two groups and received four daily i.p. injections of anti-CCL8 (n=4) or IgG (n=4). Mice were sacrificed three weeks after the final injection and the 3rd thoracic mammary glands were processed for whole mount analysis.

Histology and staining of tissues

For histological analyses, tumors were fixed in 10% formalin, paraffin-embedded and stained with hematoxylin/eosin or Elastica von Gieson (EVG) stains for light microscopy. For β-Gal staining of tissues, mammary glands, lungs from nude mice were dissected, cut into approximately 5-mm-thick pieces, fixed in 1.25% glutaraldehyde, and subjected to standard β-galactosidase staining. Tissue sections (4-μm-thick) from paraffin-embedded blocks were collected onto poly-L-lysine–coated slides and counterstained with eosin. Images shown were obtained by a Leica ICC50 HD. For whole mount staining, mammary glands were excised, spread on glass slides and after β-gal staining were fixed in Carnoy's fixative overnight at room temperature. Mammary glands were washed in 70% EtOH for 15min, gradually rehydrated in water, and stained in carmine alum overnight at room temperature. Tissues were then gradually dehydrated through serial ethanol baths, cleared in xylene and mounted with Permount. All staining experiments have been performed at least 3 times and representative results of one experiment are shown.

Statistics

Statistical analysis of the results was performed using Student's two tailed *t* test or Pearson's correlation (Microsoft Excel) as described in the text. Average values of samples are presented, error bars correspond to s.d. (<15% of mean) unless otherwise stated. Mouse survival analysis generated a Kaplan–Meier plot (CDC-Epi Info; Centers for Disease Control and Prevention, Atlanta, GA, USA), analyzed by the logrank test. A p-value of <0.05 was considered to indicate statistical significance.

Supplementary Material

Refer to Web version on PubMed Central for supplementary material.

Acknowledgments

We thank Professors I. Roninson, E. Broude and J.E. Schwarzbauer for useful comments and suggestions and F. Marini for sharing the EO771 cells.

Financial support: This study was supported by a pilot grant 5P30GM103336-02 from NIH.

References

1. Vanharanta S, Massague J. Origins of metastatic traits. Cancer Cell. 2013; 24:410–421. [PubMed: 24135279]
2. Chatzistamou I, Dioufa N, Trimis G, Sklavounou A, Kittas C, Kiaris H, et al. p21/waf1 and smooth-muscle actin alpha expression in stromal fibroblasts of oral cancers. Cell Oncol (Dordr). 2011; 34:483–488. [PubMed: 21559927]
3. Trimis G, Chatzistamou I, Politi K, Kiaris H, Papavassiliou AG. Expression of p21waf1/Cip1 in stromal fibroblasts of primary breast tumors. Hum Mol Genet. 2008; 17:3596–3600. [PubMed: 18713757]
4. Lu H, Clauser KR, Tam WL, Frose J, Ye X, Eaton EN, et al. A breast cancer stem cell niche supported by juxtacrine signalling from monocytes and macrophages. Nat Cell Biol. 2014; 16:1105–1117. [PubMed: 25266422]

5. Su S, Liu Q, Chen J, Chen F, He C, Huang D, et al. A positive feedback loop between mesenchymal-like cancer cells and macrophages is essential to breast cancer metastasis. Cancer Cell. 2014; 25:605–620. [PubMed: 24823638]
6. Condeelis J, Pollard JW. Macrophages: obligate partners for tumor cell migration, invasion, and metastasis. Cell. 2006; 124:263–266. [PubMed: 16439202]
7. Allavena P, Sica A, Solinas G, Porta C, Mantovani A. The inflammatory micro-environment in tumor progression: the role of tumor-associated macrophages. Crit Rev Oncol Hematol. 2008; 66:1–9. [PubMed: 17913510]
8. Thiery JP. Epithelial-mesenchymal transitions in tumour progression. Nat Rev Cancer. 2002; 2:442–454. [PubMed: 12189386]
9. Muller A, Homey B, Soto H, Ge N, Catron D, Buchanan ME, et al. Involvement of chemokine receptors in breast cancer metastasis. Nature. 2001; 410:50–56. [PubMed: 11242036]
10. Das S, Sarrou E, Podgrabinska S, Cassella M, Mungamuri SK, Feirt N, et al. Tumor cell entry into the lymph node is controlled by CCL1 chemokine expressed by lymph node lymphatic sinuses. J Exp Med. 2013; 210:1509–1528. [PubMed: 23878309]
11. Hollmen M, Roudnicky F, Karaman S, Detmar M. Characterization of macrophage--cancer cell crosstalk in estrogen receptor positive and triple-negative breast cancer. Sci Rep. 2015; 5:9188. [PubMed: 25776849]
12. Bae JY, Kim EK, Yang DH, Zhang X, Park YJ, Lee DY, et al. Reciprocal interaction between carcinoma-associated fibroblasts and squamous carcinoma cells through interleukin-1alpha induces cancer progression. Neoplasia. 2014; 16:928–938. [PubMed: 25425967]
13. Gong W, Howard OM, Turpin JA, Grimm MC, Ueda H, Gray PW, et al. Monocyte chemotactic protein-2 activates CCR5 and blocks CD4/CCR5-mediated HIV-1 entry/replication. J Biol Chem. 1998; 273:4289–4292. [PubMed: 9468473]
14. Islam SA, Chang DS, Colvin RA, Byrne MH, McCully ML, Moser B, et al. Mouse CCL8, a CCR8 agonist, promotes atopic dermatitis by recruiting IL-5+ T(H)2 cells. Nat Immunol. 2011; 12:167–177. [PubMed: 21217759]
15. Gong X, Gong W, Kuhns DB, Ben-Baruch A, Howard OM, Wang JM. Monocyte chemotactic protein-2 (MCP-2) uses CCR1 and CCR2B as its functional receptors. J Biol Chem. 1997; 272:11682–11685. [PubMed: 9115216]
16. Rajaram M, Li J, Egeblad M, Powers RS. System-wide analysis reveals a complex network of tumor-fibroblast interactions involved in tumorigenicity. PLoS Genet. 2013; 9:e1003789. [PubMed: 24068959]
17. Torres S, Bartolome RA, Mendes M, Barderas R, Fernandez-Acenero MJ, Pelaez-Garcia A, et al. Proteome profiling of cancer-associated fibroblasts identifies novel proinflammatory signatures and prognostic markers for colorectal cancer. Clin Cancer Res. 2013; 19:6006–6019. [PubMed: 24025712]
18. Pitteri SJ, Kelly-Spratt KS, Gurley KE, Kennedy J, Buson TB, Chin A, et al. Tumor microenvironment-derived proteins dominate the plasma proteome response during breast cancer induction and progression. Cancer Res. 2011; 71:5090–5100. [PubMed: 21653680]
19. Barbai T, Fejos Z, Puskas LG, Timar J, Raso E. The importance of microenvironment: the role of CCL8 in metastasis formation of melanoma. Oncotarget. 2015; 6:29111–29128. [PubMed: 26320180]
20. Finak G, Bertos N, Pepin F, Sadekova S, Souleimanova M, Zhao H, et al. Stromal gene expression predicts clinical outcome in breast cancer. Nat Med. 2008; 14:518–527. [PubMed: 18438415]
21. Gyorffy B, Surowiak P, Budczies J, Lanczky A. Online survival analysis software to assess the prognostic value of biomarkers using transcriptomic data in non-small-cell lung cancer. PLoS One. 2013; 8:e82241. [PubMed: 24367507]
22. Fanti P, Nazareth M, Bucelli R, Mineo M, Gibbs K, Kumin M, et al. Estrogen decreases chemokine levels in murine mammary tissue: implications for the regulatory role of MIP-1 alpha and MCP-1/JE in mammary tumor formation. Endocrine. 2003; 22:161–168. [PubMed: 14665721]
23. Chavey C, Bibeau F, Gourgou-Bourgade S, Burlinchon S, Boissiere F, Laune D, et al. Oestrogen receptor negative breast cancers exhibit high cytokine content. Breast Cancer Res. 2007; 9:R15. [PubMed: 17261184]

24. Fenner J, Stacer AC, Winterroth F, Johnson TD, Luker KE, Luker GD. Macroscopic stiffness of breast tumors predicts metastasis. Sci Rep. 2014; 4:5512. [PubMed: 24981707]
25. Bouquet F, Pal A, Pilones KA, Demaria S, Hann B, Akhurst RJ, et al. TGFbeta1 inhibition increases the radiosensitivity of breast cancer cells in vitro and promotes tumor control by radiation in vivo. Clin Cancer Res. 2011; 17:6754–6765. [PubMed: 22028490]
26. Van Damme J, Proost P, Lenaerts JP, Opdenakker G. Structural and functional identification of two human, tumor-derived monocyte chemotactic proteins (MCP-2 and MCP-3) belonging to the chemokine family. J Exp Med. 1992; 176:59–65. [PubMed: 1613466]
27. Blaszczyk J, Coillie EV, Proost P, Damme JV, Opdenakker G, Bujacz GD, et al. Complete crystal structure of monocyte chemotactic protein-2, a CC chemokine that interacts with multiple receptors. Biochemistry. 2000; 39:14075–14081. [PubMed: 11087354]
28. Roussos ET, Condeelis JS, Patsialou A. Chemotaxis in cancer. Nat Rev Cancer. 2011; 11:573–587. [PubMed: 21779009]
29. Chen J, Yao Y, Gong C, Yu F, Su S, Liu B, et al. CCL18 from tumor-associated macrophages promotes breast cancer metastasis via PITPNM3. Cancer Cell. 2011; 19:541–555. [PubMed: 21481794]
30. Casey AE, Laster WR Jr, Ross GL. Sustained enhanced growth of carcinoma EO771 in C57 black mice. Proc Soc Exp Biol Med. 1951; 77:358–362. [PubMed: 14854049]
31. Skarnes WC, Rosen B, West AP, Koutsourakis M, Bushell W, Iyer V, et al. A conditional knockout resource for the genome-wide study of mouse gene function. Nature. 2011; 474:337–342. [PubMed: 21677750]
32. Carmeliet P, Jain RK. Angiogenesis in cancer and other diseases. Nature. 2000; 407:249–257. [PubMed: 11001068]
33. Rafii S, Avecilla ST, Jin DK. Tumor vasculature address book: identification of stage-specific tumor vessel zip codes by phage display. Cancer Cell. 2003; 4:331–333. [PubMed: 14667498]
34. Cristofanilli M, Hayes DF, Budd GT, Ellis MJ, Stopeck A, Reuben JM, et al. Circulating tumor cells: a novel prognostic factor for newly diagnosed metastatic breast cancer. J Clin Oncol. 2005; 23:1420–1430. [PubMed: 15735118]
35. Riethdorf S, Fritsche H, Muller V, Rau T, Schindlbeck C, Rack B, et al. Detection of circulating tumor cells in peripheral blood of patients with metastatic breast cancer: a validation study of the CellSearch system. Clin Cancer Res. 2007; 13:920–928. [PubMed: 17289886]
36. Kim MY, Oskarsson T, Acharyya S, Nguyen DX, Zhang XH, Norton L, et al. Tumor self-seeding by circulating cancer cells. Cell. 2009; 139:1315–1326. [PubMed: 20064377]
37. Hu B, Castillo E, Harewood L, Ostano P, Reymond A, Dummer R, et al. Multifocal epithelial tumors and field cancerization from loss of mesenchymal CSL signaling. Cell. 2012; 149:1207–1220. [PubMed: 22682244]
38. Pienta KJ, Machiels JP, Schrijvers D, Alekseev B, Shkolnik M, Crabb SJ, et al. Phase 2 study of carlumab (CNTO 888), a human monoclonal antibody against CC-chemokine ligand 2 (CCL2), in metastatic castration-resistant prostate cancer. Invest New Drugs. 2013; 31:760–768. [PubMed: 22907596]
39. Sandhu SK, Papadopoulos K, Fong PC, Patnaik A, Messiou C, Olmos D, et al. A first-in-human, first-in-class, phase I study of carlumab (CNTO 888), a human monoclonal antibody against CC-chemokine ligand 2 in patients with solid tumors. Cancer Chemother Pharmacol. 2013; 71:1041–1050. [PubMed: 23385782]

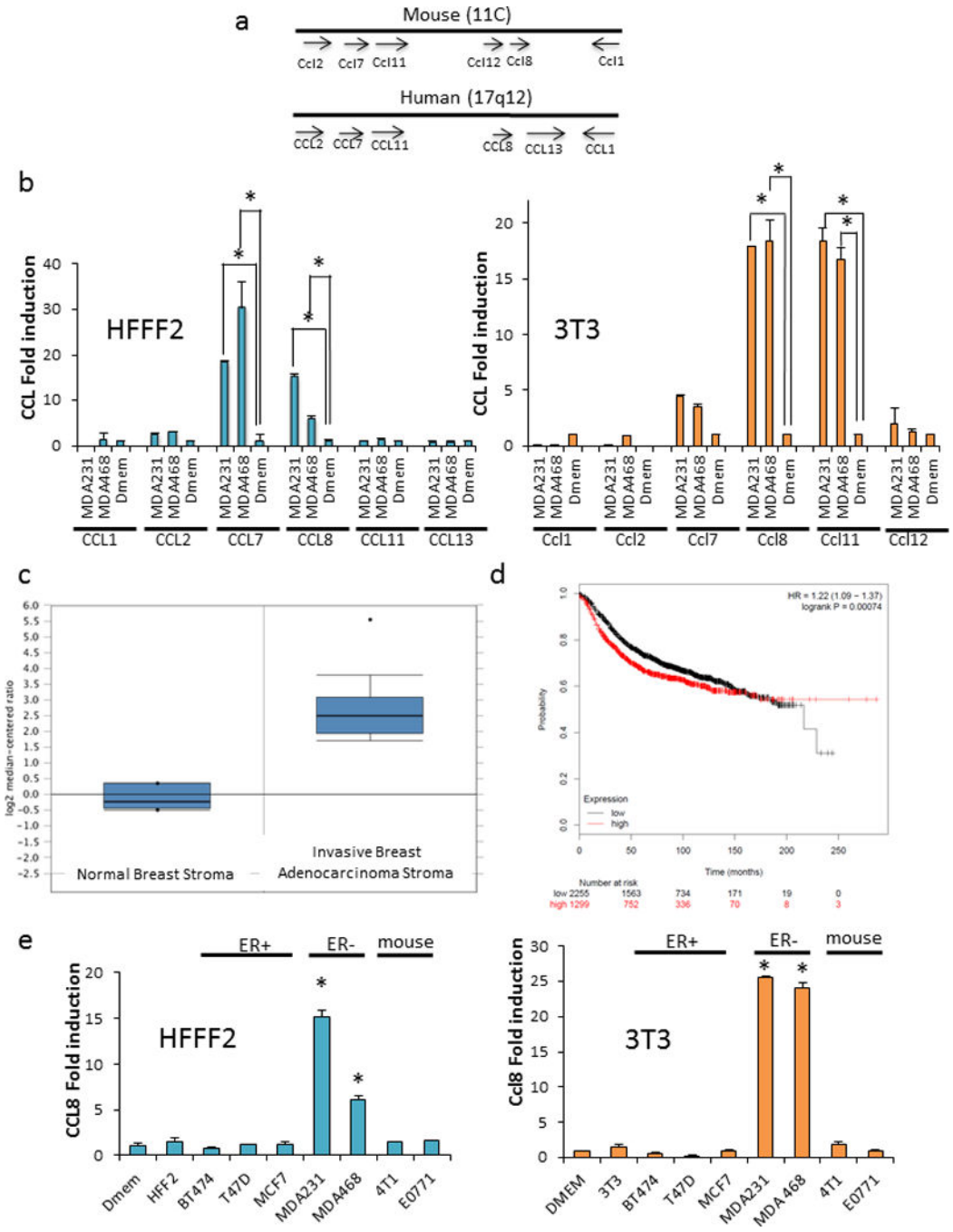

Figure 1.

Establishment of a self-sustained CCL8 gradient between breast cancer and stromal cells. **(a)** Genomic organization of the cytokine cluster that harbors Ccl8 in mouse and humans. Data were compiled from Ensembl Genome Browser (www.ensembl.org). **(b)** Cytokine expression in human HFFF2 and mouse 3T3 fibroblasts following culture in MDA231 and MDA468 breast cancer cell conditioned media. Ccl8 is the only cytokine in this cluster that specifically responds to breast cancer cells' media in both mouse and human fibroblasts. **(c)** Expression of CCL8 in human invasive breast cancer stroma. Data were obtained by

Oncomine, https://www.oncomine.org. **(d)** Breast cancer patients' survival in relation to CCL8 expression. High CCL8 expression is associated with worse prognosis. Data were obtained from Kaplan-Meier-plotter [Breast Cancer], www.kmplot.com/. High expression is indicated in red, low expression in blue, cutoffs were set automatically by the software. **(e)** Ccl8 expression in mouse and human fibroblasts following exposure to breast cancer cells' conditioned media. *, $p<0.01$, Student's t-test.

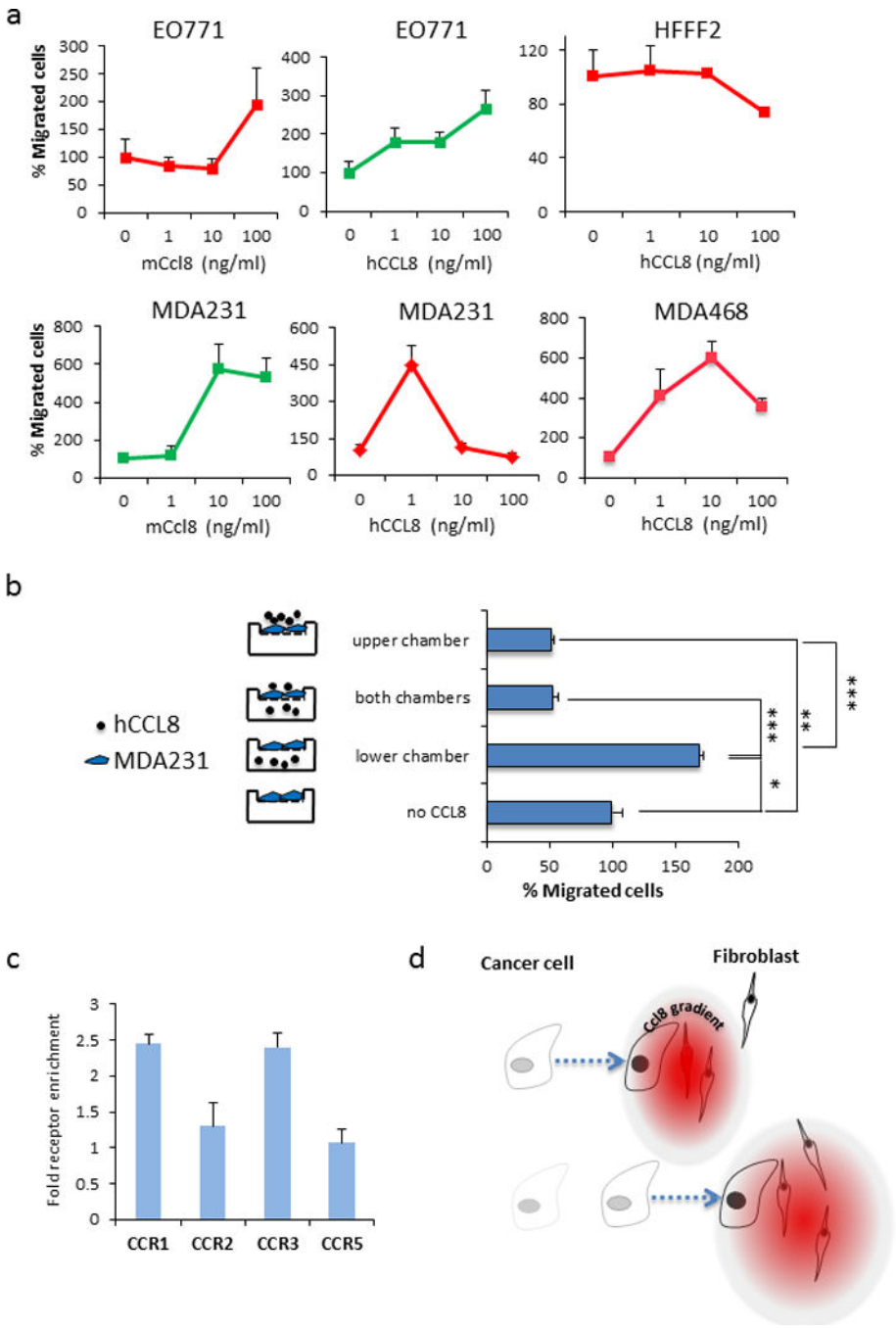

Figure 2.

CCL8-induced chemoattraction. **(a)** Chemoattraction of various breast cancer cells and fibroblasts by increasing amounts of CCL8 in transwells *in vitro*. **(b)** MDA231 cells' migration in response to CCL8 added in the upper or lower chamber of the transwells or distributed evenly between the upper and the lower chamber. **(c)** Receptors' expression measured by quantitative PCR in cells migrated through the transwells relative to receptors expression in regular wells **(c)** Diagrammatic depiction of the CCL8 gradient (red) that

originates from the fibroblasts in response to signals from the cancer cells. *, p=0.05, **, p<0.05, ***, p<0.001 Student's t-test.

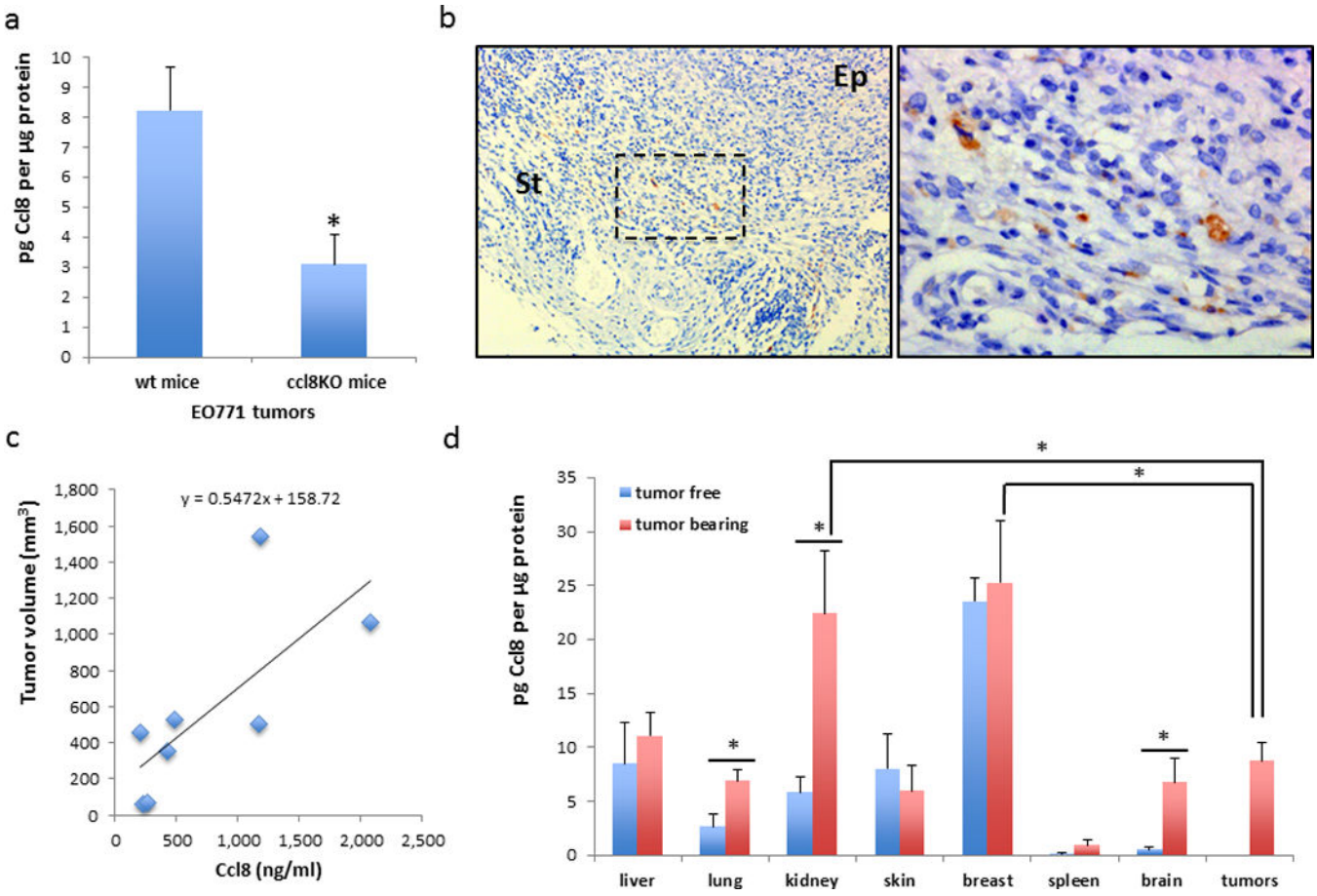

Figure 3.

Ccl8 expression in tumors, stroma and peripheral tissues. **(a)** Ccl8 levels of EO771 tumors developed in wt (n=6) and Ccl8KO (n=4) mice. Tumor volumes in all cases analyzed ranged between 200mm^3–300mm^3. **(b)** Expression of Ccl8 in the stroma of EO771 tumors growing in wt mice. Right panel shows in higher magnification of the area marked in the left panel by a blue square. **(c)** Serum Ccl8 levels in relation to tumor volume in different EO771 breast cancer – bearing mice. Ep, epithelium, St, fibroblastic stroma. $p<0.05$, Pearson's correlation **(d)** Tumoral Ccl8 (n=6) and Ccl8 in various organs from tumor free (n=4) and mice bearing EO771 tumors (n=5) (200mm^3–300mm^3). *, $p<0.05$ Student's t-test

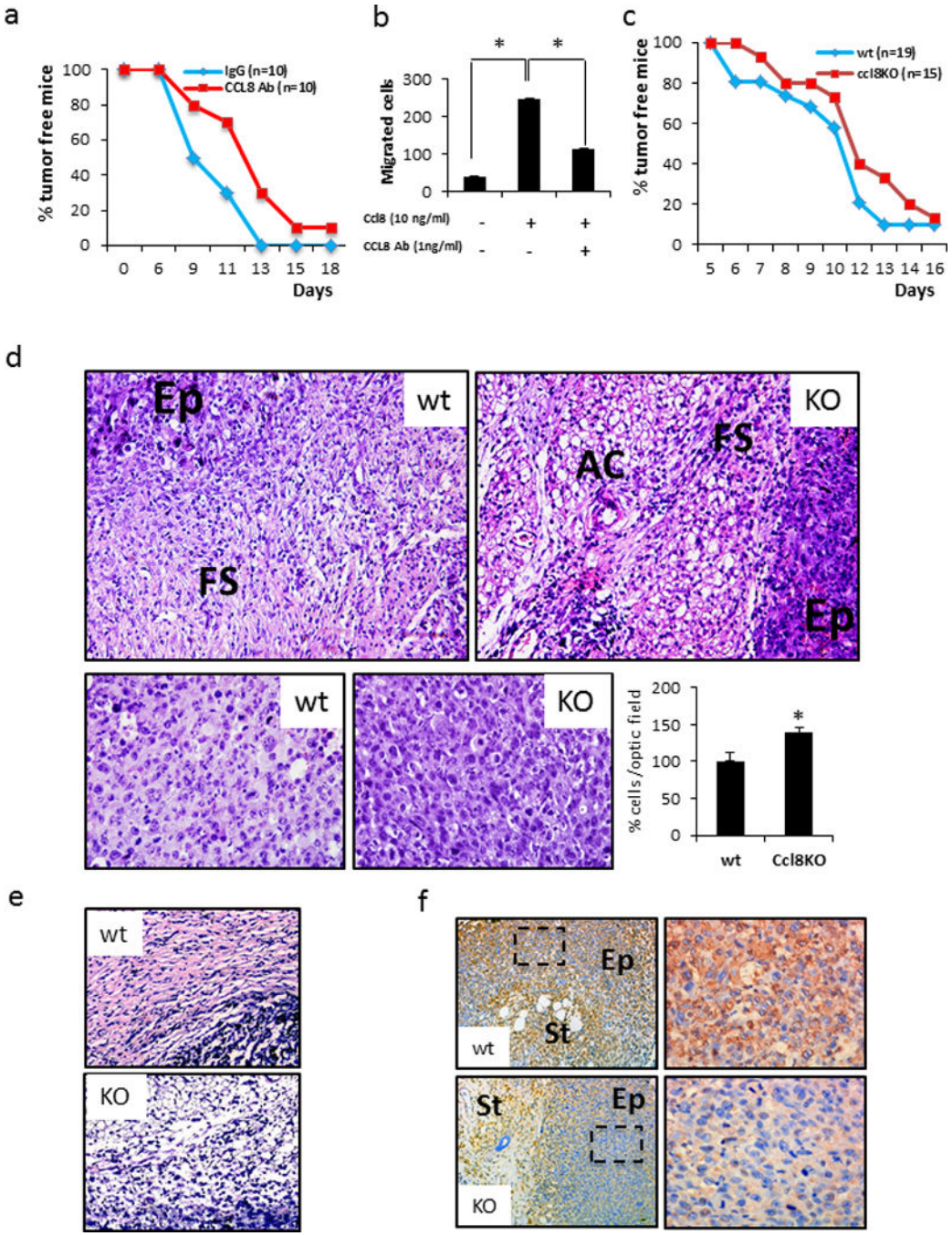

Figure 4.

Effect of Ccl8 inhibition in EO771 tumors *in vivo*. **(a)** EO771 tumor onset in wt mice following administration of a neutralizing antibody for CCL8. **(b)** Inhibition of mCcl8-induced chemoattraction by a neutralizing antibody for CCL8 in RAW 264.7 macrophages in transwells. **(c)** EO771 tumor onset in wt and Ccl8KO mice (24). **(d)** Histology of EO771 tumors in wt and Ccl8KO mice. Genotypes are shown in white insets. The upper panel corresponds to images from the core of the tumor while the lower panel from the margins. Lower right graph indicates cellularity expressed as epithelial cells per high power optic

field. (n=3 per genotype). Ep, epithelium, FS, fibroblastic stroma, AC, antipocytic stroma. *, ($p<0.05$,Student's t-test). **(e)** Van Gieson staining of EO771 tumors in control and Ccl8KO mice. **(f)** Vimentin expression (brown staining) close to tumor margins in EO771 tumors that developed in wt and Ccl8KO mice. Right panel shows in higher magnification of the area marked in the left panel by a black square.

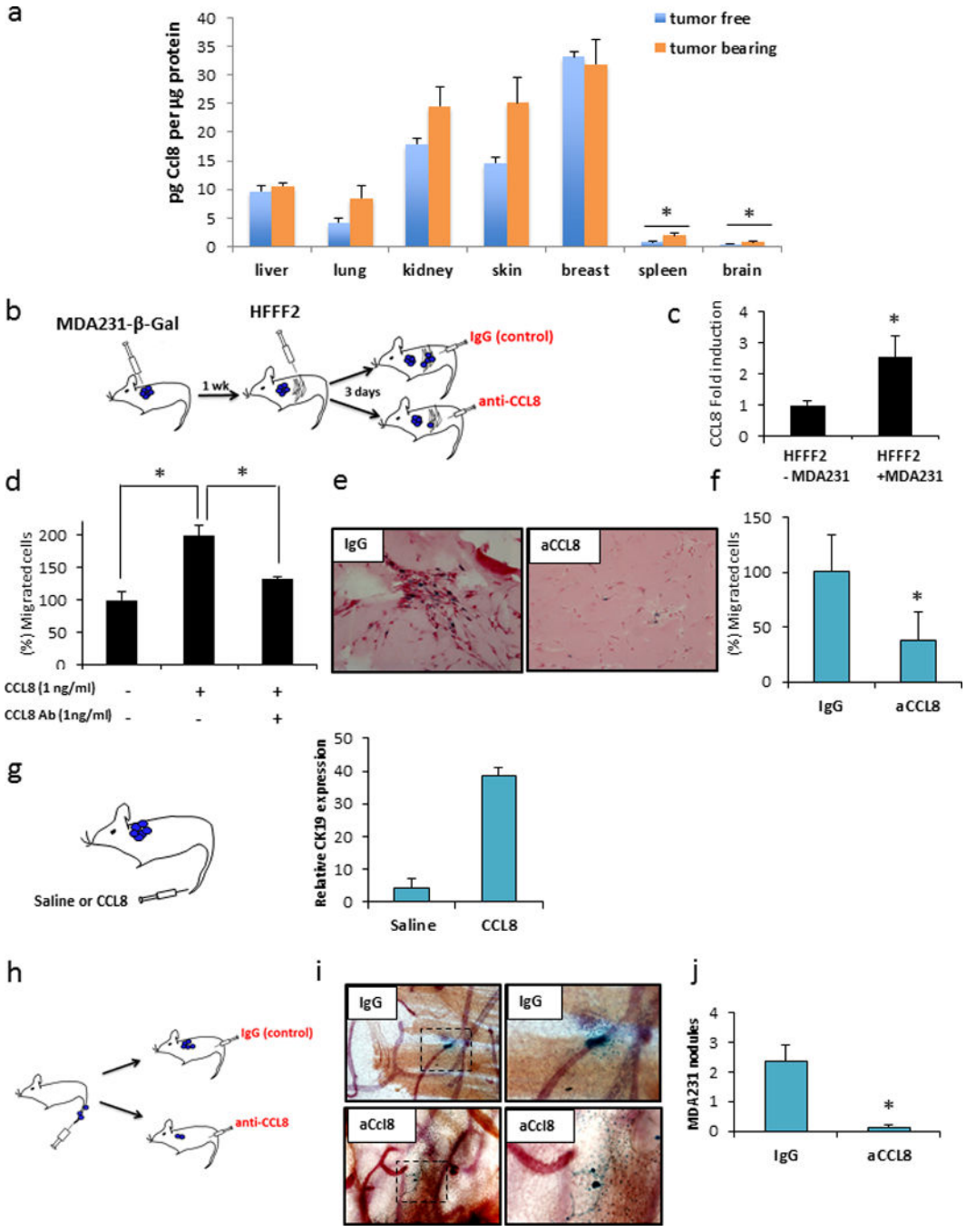

Figure 5.

Modulation of CCL8 levels in mice affects the metastatic potential of MDA231 cells. **(a)** Ccl8 in various organs from tumor free (n=3) and mice bearing MDA231 tumors (n=3) (200mm^3–300mm^3). **(b)** Diagrammatic illustration of the experimental design. **(c)** Expression of CCL8 in matrigel-enclosed fibroblasts inoculated adjacent (about 5mm) to MDA231 tumors or in tumor-free mice (control) (n=3). **(d)** Inhibition of CCL8-induced chemoattraction by a neutralizing antibody for hCCL8 in MDA231 cells in transwells. **(e)** Invasion of MDA231-β-Gal cells (blue) in matrigel-enclosed HFFF2 fibroblasts inoculated

in nude mice and treated daily for 3 days with neutralizing antibody for CCL8 (aCCL8) (n=5) or IgG (n=4). Sections were counterstained with eosin. Samples from Ab-treated mice exhibited consistently minimal invasion of MDA231 cells while controls had variable invasion of MDA231 cells. Quantification of fibroblasts in control and Ab-treated mice is shown in **(f). (g)** CTCs' abundance, in arbitrary units, 24h after they received CCL8 (n=2) or saline (n=2). **(h)** Diagrammatic illustration of the experimental process followed to reveal the effects of CCL8 inhibition in the seeding of mammary glands from MDA231-β-Gal cells. **(i)** Representative images of MDA231-β-Gal cells colonizing the mammary glands of mice that received IgG (n=4) or aCCL8 (n=4). Right panel shows the area indicated in dashed square in high magnification. Quantification of the MDA231-β-Gal foci in control and Ab-treated mice is shown in **(j)**.

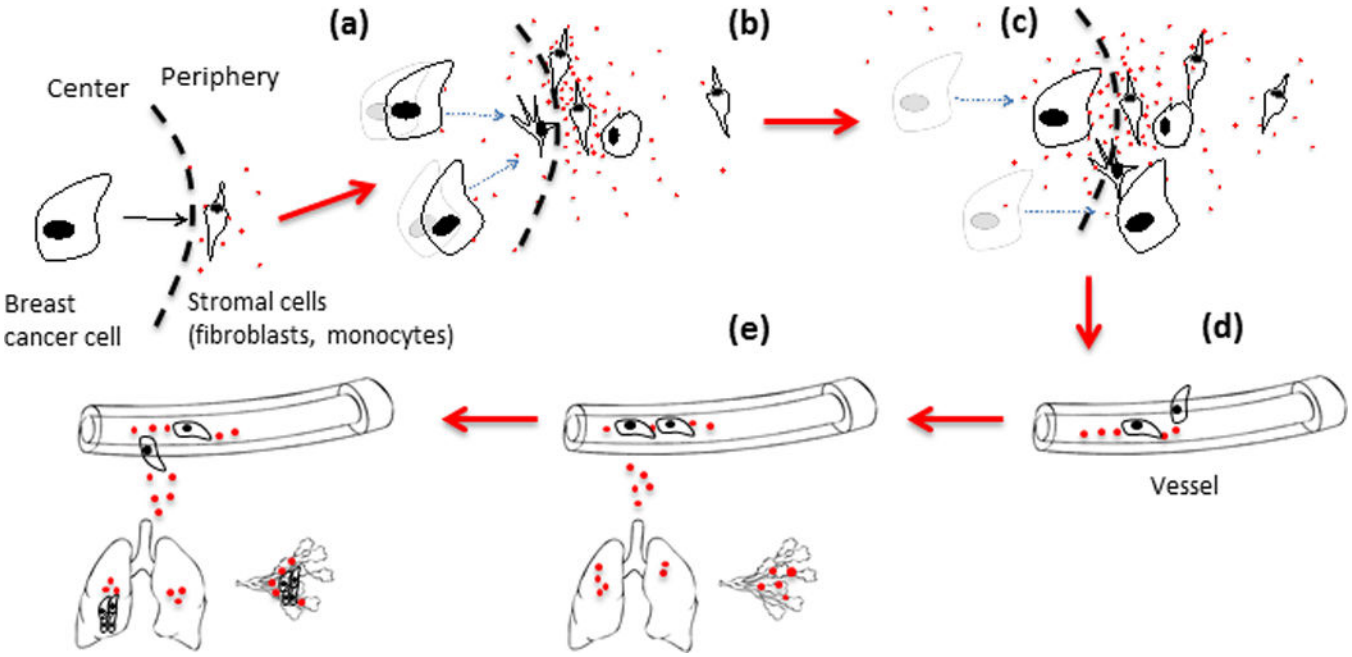

Figure 6.

Diagrammatic illustration of how a gradient of CCL8 is self-sustained to promote dissemination of breast cancer cells. Fibroblasts and probably other stromal cells are activated in response to secreted factors produced by the breast cancer cells **(a)** and activate CCL8 expression which results in the establishment of a CCL8-gradient **(b)**. This results in the chemoattraction of the cancer cells towards the CCL8 gradient casing progressively their movement along with the shift of the gradient towards the tumor margins at which stromal cells are more abundant **(c)**. Eventually cancer cells intravasate in response to elevated levels of CCL8 in circulation establishing CTC populations **(d)**. Ultimately, niches of increased CCL8 production in peripheral tissues promote the extravasation of cancer cells and the establishment of populations of secondary tumor growth **(e)**.

Table 1

Primers used for Real-time quantitative PCR

Gene	Forward Primer	Reverse Primer
Human CCL1	AATACCAGCTCCATCTGCTCCAA	GAACCCATCCAACTGTGTCCAAG
Human CCL2	CAGCCAGATGCAATCAATGC	GCACTGAGATCTTCCTATTGGTGAA
Human CCL7	CACTTCTGTGTCTGCTGCTCAC	GTTTTCTTGTCCAGGTGCTTCATA
Human CCL8	AGATGAAGGTTTCTGCAGCGC	TGGAAACTGAATCTGGCTGAG
Human CCL11	ACACCTTCAGCCTCCAACAT	GGTCTTGAAGATCACAGCTT-
Human CCL13	CGTCCCATCTACTTGCTGCT	CTTCAGGGTGTGAGCTTTCC
Human keratin 19	GCGGGACAAGATTCTTGGTG	CTTCAGGCCTTCGATCTGCAT
Human CCR1	TTTGGTGTCATCACCAGCAT	GCCTGAAACAGCTTCCACTC
Human CCR2	TGGCTGTGTTTGCTTCTGTC	TTCCCGAGTAGCAGATGACC
Human CCR3	TCGTTCTCCCTCTGCTCGTT	GCCGGATGGCCTTGTACTTT
Human CCR5	TAGTCATCTTGGGGCTGGTC	TGTAGGGAGCCCAGAAGAGA
Mouse GAPDH	ACCCAGAAGACTGTGGATGG	CACATTGGGGGTAGGAACAC
Mouse Ccl1	AAGATGGGCTCCTCCTGTCC	TTGAGGCGCAGCTTTCTCTAC
Mouse Ccl2	AGGTCCCTGTCATGCTTCTG	TCTGGACCCATTCCTTCTTG
Mouse Ccl7	AATGCATCCACATGCTGCTA	CTTTGGAGTTGGGGTTTTCA
Mouse Ccl8	TTCCAGCTTTGGCTGTCTCT	GGGTGCTGAAAAGCTACGAG
Mouse Ccl11	GATCTTCTTACTGGTCATGATAAAGCA	TGTCTCCCTCCACCATGCA
Mouse Ccl12	GTCCTCAGGTATTGGCTGGA	GGGTCAGCACAGATCTCCTT